

AutoRAN: Automated and Zero-Touch Open RAN Systems

Stefano Maxenti, *Student Member, IEEE*, Ravis Shirkhani, *Student Member, IEEE*,
Maxime Elkael, *Member, IEEE*, Leonardo Bonati, *Member, IEEE*, Salvatore D’Oro, *Member, IEEE*,
Tommaso Melodia, *Fellow, IEEE*, Michele Polese, *Senior Member, IEEE*

Abstract—Modern cellular networks adopt a software-based and disaggregated approach to support diverse requirements and mission-critical reliability needs. While software-based approaches introduces flexibility, it also increases the complexity of the network architectures, which calls for robust automation frameworks that can deliver efficient and fully-autonomous configuration, scalability, and multi-vendor integration. This paper presents AutoRAN, an automated, intent-driven framework for zero-touch provisioning of open, programmable cellular networks. Leveraging cloud-native principles, AutoRAN employs virtualization, declarative infrastructure-as-code templates, and disaggregated micro-services to abstract physical resources and protocol stacks. Its orchestration engine integrates Large Language Models (LLMs) to translate high-level intents into machine-readable configurations, enabling closed-loop control via telemetry-driven observability. Implemented on a multi-architecture OpenShift cluster with heterogeneous compute (x86/ARM CPUs, NVIDIA GPUs) and multi-vendor Radio Access Network (RAN) hardware (Foxconn, NI), AutoRAN automates deployment of O-RAN-compliant stacks—including OpenAirInterface, NVIDIA ARC RAN, Open5GS core, and O-RAN Software Community (OSC) RIC components—using Continuous Integration and Continuous Delivery/Deployment (CI/CD) pipelines. Experimental results demonstrate that AutoRAN is capable of deploying an end-to-end Private 5G network in less than 60 seconds with 1.6 Gbps throughput, validating its ability to streamline configuration, accelerate testing, and reduce manual intervention with similar performance than non cloud-based implementations. With its novel LLM-assisted intent translation mechanism, and performance-optimized automation workflow for multi-vendor environments, AutoRAN has the potential of advancing the robustness of next-generation cellular supply chains through reproducible, intent-based provisioning across public and private deployments.

Index Terms—O-RAN, Open RAN, Automation, Testing, Zero-touch, 5G, 6G

I. INTRODUCTION

Today’s cellular networks serve a variety of customers and use cases with heterogeneous deployments and technologies that operate under diverse user requirements and channel conditions [1]. This diversity of requirements and strategic support for society and economy make cellular networks extremely complex systems. For instance, an end-to-end deployment of

a 5th generation (5G) cellular system counts tens of micro-services for the core network, a distributed Radio Access Network (RAN) with a disaggregated protocol stack capable of handling hundreds of users from a single base station, and additional services for management and optimization of the network [2].

Even carrier networks, where operators bear the know-how to manage and control such systems, suffer from outages and anomalies due to the complex nature of cellular networks [3]. This major pain point is further exacerbated in private 5G networks, often operated by enterprise Information Technology (IT) departments, which face challenges in reliably planning, deploying, operating, and scaling private connectivity solutions. Compared to Wi-Fi, which is usually deployed as integrated solution with simple and inexpensive access points, private cellular systems can provide the necessary performance guarantees to enable mission-critical use cases, and deliver the ultra-low latency and high throughput connectivity needed for enabling Industry 4.0 and automation [4]. On the other hand, cellular systems require expert knowledge and a more involved management and monitoring effort. For this reason, enterprise often resorts to system integrators, which streamline the deployment and management process but add an intermediate layer between the network and the enterprise. This also increases integration costs [5] and reduces the ability to customize the network. Part of this complexity also stems from the recent transition of cellular systems to software-based and disaggregated architectures such as Cloud RAN (CRAN), Virtualized RAN (vRAN) and Open RAN. Indeed, this transition brings flexibility and programmability, as well as support for multi-vendor deployments. However, the decoupling of RAN elements results in an increased number of network functions (e.g. Radio Unit (RU), Distributed Unit (DU) and Central Unit (CU) in a disaggregated Next Generation Node Base (gNB)) that add complexity to the network and call for proper automation tools capable of taming such complexity. Indeed, while Continuous Integration (CI)/Continuous Deployment (CD) and automation are widely used in cloud solutions, existing techniques cannot be directly applied to cellular systems due to challenges involving radio transmissions, spectrum allocation policies, distributed deployments, core and RAN elements for low latency, high throughput, and the support of the real-time processing for wireless signals. Notably, generic cloud platforms assume best-effort workloads and lack support for RAN-specific requirements such as CPU pinning, nanosecond clock synchronization, and specialized networking.

S. Maxenti, R. Shirkhani, M. Elkael, L. Bonati, T. Melodia, and M. Polese are with the Institute for the Wireless Internet of Things, Northeastern University, Boston, MA, U.S.A. E-mail: {maxenti.s, shirkhani.r, m.elkael, l.bonati, melodia, m.polese}@northeastern.edu. Salvatore D’Oro is with zTouch Networks, Inc., Boston, MA, U.S.A. Email: salvo@ztouchnet.com.

This work was partially supported by the National Telecommunications and Information Administration (NTIA)’s Public Wireless Supply Chain Innovation Fund (PWSCIF) under Award No. 25-60-IF054 and by the U.S. National Science Foundation under grant CNS-2117814.

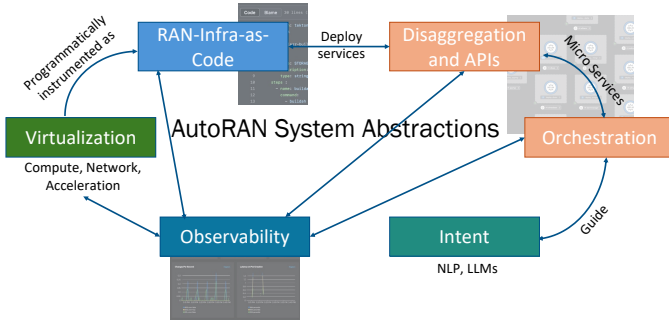


Fig. 1: Key abstractions for the AutoRAN system.

In this paper, we address the above challenges and propose, design, and develop AutoRAN, an automated and intelligent framework for zero-touch configuration and provisioning of open and programmable cellular networks. AutoRAN extends cloud-native abstractions to provide support for RAN-specific workloads, with automation and virtualization that extend from the core network to the cell site.

The AutoRAN design (Figure 1) is based on key abstractions and capabilities: (i) the physical infrastructure is abstracted through virtualization of networking, hardware accelerators, and compute resources. This is programmatically configured and operationalized using a (ii) declarative approach, where code and templates are used to describe the characteristics and configuration of the system, enabling versioning control, automated configuration roll-outs, and end-to-end optimization of infrastructure parameters. The applications, which in this case are RAN-related workloads, are deployed as (iii) disaggregated micro-services, coexisting on the same infrastructure as traditional IT and cloud deployments, while exposing Application Programming Interfaces (APIs) for reconfiguration, interaction across services, and telemetry. For example, a base station is split into multiple micro-services (i.e., DU and CU) connected through open interfaces. The service life-cycle is managed through (iv) end-to-end orchestration to automatically converge to a valid set of services with the appropriate status and configuration across software applications and infrastructure. The orchestrator is guided by (v) high-level intents for operator requirements (e.g., coverage area, minimum Quality of Service (QoS) level) and translated into machine-readable configurations through Natural Language Processing (NLP) and Large Language Models (LLMs). Finally, (vi) observability makes it possible to track the end-to-end system status and coordinate with the orchestrator to implement closed-loop control.

We designed and implemented a system that abides by such principles on a fully-programmable OpenShift cluster [6] with heterogeneous compute architectures, accelerators, and end-to-end components for the software stacks. Specifically, we design a RAN-Infrastructure-as-Code solution that, based on an intent expressed by the user through an LLM prompt, deploys and configures gNB on a cluster with 13 nodes with x86 and ARM Central Processing Units (CPUs), NVIDIA L40, A100, and GH200 Graphics Processing Units (GPUs), and radios from various radio manufacturers (Foxconn and NI/Ettus). The system automation combines OpenShift, Tekton pipelines, ArgoCD, and similar tools to automatically deploy an optimized RAN based on OpenAirInterface (OAI) [7], [8], on NVIDIA

ARC-OTA [9], [10], or on srsRAN [11], core network based on Open5GS, and RAN Intelligent Controller (RIC) components from the O-RAN Software Community (OSC). Once the system is deployed, the automation framework orchestrates end-to-end performance and functional tests. We show how to transition from generic bare metal deployments to integrated and automated deployments on clusterization platforms.

Overall, the contributions of our paper are as follows:

- Conceptualize, implement and evaluate AutoRAN, an end-to-end automation solution for zero-touch deployment, configuration and testing of multi-vendor cellular networks, taking advantage of hardware accelerators integrated into a cloud computing platform;
- We efficiently integrate various RAN stacks into a unified computing and automation platform, introducing advanced virtualization techniques and showing RAN coexistence with generic cloud computing software;
- Automate deployment and testing with AutoRAN to achieve an end-to-end deployment in less than 60 seconds and peak throughput of 1.6 Gbps on the cloud-based AutoRAN infrastructure;
- Design and develop an LLM pipeline that converts high-level intents into verifiable and bespoke cluster configuration and RAN deployment policies;
- Extensively profile AutoRAN performance on different tasks, including deploying and testing cellular networks.

The remainder of this paper is organized as follows. In Section II, we review literature works related to ours. In Section III, we discuss the foundational design principles behind AutoRAN, while in Section IV we discuss the implementation of such principles on the cluster infrastructure. In Section V, we focus on the automation workflows for deployment and testing and describe the design and training procedures of our LLM. Finally, in Section VI, we provide results and metrics, while in Section VII, we draw our conclusions and discuss future works.

II. RELATED WORK

AutoRAN proposes a solution to automatically configure, deploy, and operate a multi-vendor Open RAN system. It also provides a convenient way to perform repeatable tests with different specifications, and deployment through a LLM interface. The work encompasses various aspects of configuring infrastructure for automated deployment and testing of Open RAN while investigating Artificial Intelligence (AI) applications in telecommunications.

The authors of [12] introduce an enterprise-scale Open RAN testbed that enables realistic, high-fidelity research. By automating Open RAN deployment and real-time telemetry collection, they aim at enabling testing and optimization of network functions. NeutRAN [13] provides zero-touch multi-tenancy through RAN/spectrum sharing on OpenShift, dynamically allocating resources via optimization rApps for efficient utilization. Similarly, 5G-CT [14] automates end-to-end (E2E) 5G/O-RAN networks using OpenShift and GitOps workflows, integrating capabilities for the continuous integration, deployment, and testing with OAI, commercial core, and

Software-defined Radios (SDRs). 5GShell [15] aims at reducing human-based network configurations by providing a plug-and-play framework designed to automate the deployment of 5G cellular networks. It enables users to deploy different cores, two different protocol stacks, and softwarized User Equipment (UE). A demo of cloud-native 5G network automation using Kubernetes and OpenShift operators is presented in [16]. This solution automates deployment, configuration, service upgrade, and switching between monolithic and disaggregated RAN architectures based on network traffic. Although these works focus on automating cloud computing and virtualization for Open RAN, they do not include hardware accelerators such as NVIDIA GPUs in the infrastructure. AutoRAN, instead, has a more diverse and heterogeneous infrastructure both for RUs and gNB stacks, and is built with cloud-computing automation and scalability in mind.

RAN accelerators are instead considered in [9], [17]. X5G [9] is an open, programmable, and multi-vendor private 5G testbed that integrates NVIDIA GPUs to accelerate the 5G physical layer interfacing with OAI for high-DU. CloudRIC [17], is a virtualized O-RAN solution that reduces cost and improves energy efficiency by pooling hardware accelerators such as NVIDIA GPUs and FPGAs across multiple DUs. Although these works showcase the advantages of using accelerators in improving the performance of RAN deployments, they do not focus on automating the configurations of the infrastructure, and are limited to simple and non-scalable deployments mostly based on bare-metal implementations.

From the orchestration perspective, SoftRAN [18] introduces a software-defined model that replaces the traditional distributed control plane with a logically centralized controller, which improves the global network optimization, management, scalability, and coordination. OrchestRAN [19] proposes optimized allocations of resources to gNBs varying from edge to cloud. ATHENA [20], instead, is a cloud-native, multi-x network management and orchestration framework for the automation of network workloads lifecycle. It has a declarative, intent-based, and multi-vendor-compatible software-defined architecture that aims at improving the network management flexibility. [21] proposes a cloud-based federation framework that automates testbed integration, resource sharing, and remote experimentation on Amazon Web Services. It supports heterogeneous testbeds, allowing seamless access to distributed research infrastructure. Building on these efforts to automate and virtualize Open RAN infrastructure, recent research has begun to explore the role of LLMs in further simplifying and streamlining network configuration and management. Some works explore solutions to automatically produce network configurations using language models [22]. Others focus on mobile radio network and 5G deployments, e.g., [23], where the authors analyze various applications for domain knowledge, code and network configuration generation.

Compared to these works, which focus on features such as acceleration, orchestration, automation, or LLMs, AutoRAN provides a holistic approach that covers all aspects of deployment and testing of a cellular network. It is also the first solution to simplify cellular network operations and management by enabling the intent-based deployment of network workloads

and tests on a heterogeneous infrastructure with accelerators, different CPU architectures, and multi-vendor 5G software and radio devices.

III. AUTORAN CLOUD-NATIVE DESIGN

In this section, we discuss the design of AutoRAN, focusing on the foundational principles that we leveraged to introduce zero-touch automation in E2E software-driven cellular networks (Figure 1). Specifically, we review how virtualization, RAN-Infrastructure-as-Code, disaggregation and micro-services, orchestration, intent-based configuration, and observability are leveraged in AutoRAN, whose high-level architecture is shown in Figure 2.

The systems and services that are required for 5G networks combine (i) elastic workloads, for core network, orchestration, and management-related services; and (ii) the RAN, which has stringent performance guarantees requirements to run complex Digital Signal Processing (DSP). Due to their nature, elastic workloads can be placed directly on the infrastructure (e.g., at the edge, or in the cloud) with the caveat that connectivity and latency requirements are satisfied (e.g., a core network may run in cloud data centers such as AWS or Azure as long as the latency to reach the cloud is not too high). As shown in Figure 2 (light blue), these include components for the core network, RICs, and various non-latency-sensitive Machine Learning (ML) applications. In contrast, RAN workloads (dark blue in Figure 2) need to be distributed to edge or cell site locations, close to the end users, to satisfy the high data rates and predictable low latency requirements needed by RAN functions [24]. For instance, the deployment of a gNB—which comprises the disaggregated elements CU, DU, and RU—requires that DU and RU are in close proximity to minimize latency over the front-haul interface carrying high-capacity traffic related to I/Q streams. Additionally, DUs at cell sites might also need to host low-latency control and sensing applications such as dApps [25], [26], [27]. These might perform spectrum sensing, beam management, anomaly detection or channel estimation, which need direct access to real-time I/Q sample streams, which calls for edge deployments rather than cloud ones due to the high-capacity bandwidth requirement to transmit I/Q streams.

Figure 2 shows how AutoRAN leverages a fast and programmable network to implement the fronthaul interface between the DU and multiple options as radios, including commercial RUs, RU emulators, and software-defined radios. To holistically manage and optimize such a diverse architecture, AutoRAN implements automated workflows for infrastructure configuration, E2E deployment, and testing, based on the following design principles.

A. Abstracting Compute, Networking, and Acceleration

As we discuss in Section IV, AutoRAN is built on top of an infrastructure with a diverse set of compute, networking, and acceleration resources. To manage this complexity and diversity, we design AutoRAN to abstract each individual component of the infrastructure via virtualization, thus creating a homogeneous software layer that hides the details of the underlying infrastructure to simplify deployment and control. At the

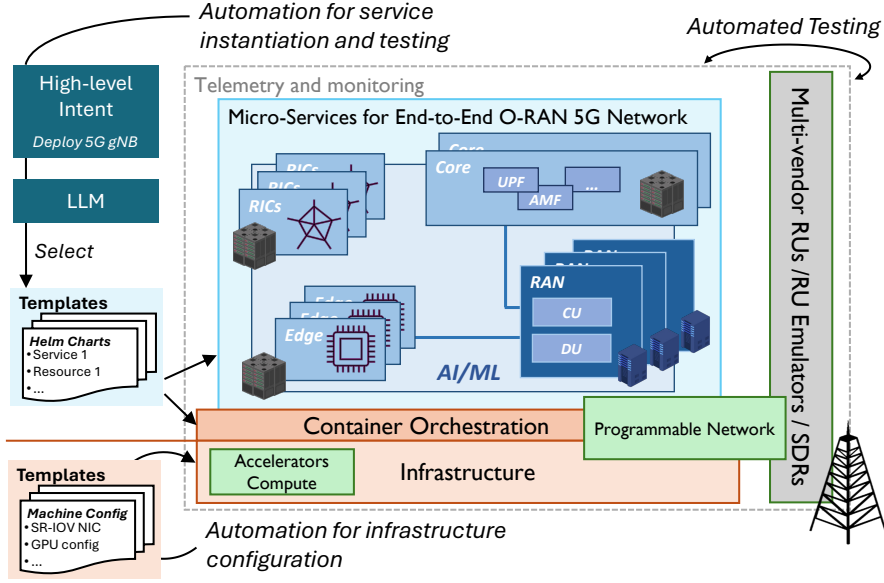


Fig. 2: AutoRAN architecture and foundational components.

same time, we configure the infrastructure nodes and software (e.g., through proper kernel profiles) so that the virtualization overhead does not compromise the performance compared to bare metal, non-virtualized setups, as shown in Section VI-D2. We leverage Podman as the base container technology for OpenShift, and rely on Single Root I/O Virtualization (SR-IOV) to virtualize the Network Interface Card (NIC) and enable multiplexing of different traffic flows on the same interface. GPUs are presented to the workloads through the NVIDIA Docker plugin for GPUs, which makes sure that containers can fully access their compute capabilities. Finally, to account for different CPU architectures and guarantee optimized performance of CPU operations, we avoid translating instructions and develop a native, multi-architecture build pipeline that accounts for both ARM and x86.

Further, the infrastructure is organized as a cluster, i.e., an abstraction where compute nodes work under a centralized control plane (e.g., an orchestrator as in Section III-D), rather than as isolated servers. Combined with virtualization, this approach simplifies deployment and management by replicating configurations across nodes, supports heterogeneous computing, and enables on-demand reconfiguration. Applications can migrate between equivalent nodes for load balancing. Moreover, it allows for a logical separation of data and application logic, e.g., to provide resilient and dynamic RAN services with storage for state and configurations that persists the life cycle of individual services.

B. Declarative Approach for RAN-Infrastructure-as-Code

As discussed above, the AutoRAN cluster combines a heterogeneous set of compute, acceleration, and networking components, and additional abstractions on top of it. The system needs to go through multiple stages for the configuration: (i) at pre-deployment, for planning (i.e., day 0); (ii) at deployment, i.e., whenever new devices or services need to be added or for updates (i.e., day 1); and (iii) for post-deployment, to manage

the complete life-cycle (day 2). Manually configuring the cluster infrastructure and software is a task that is time consuming, prone to errors, and lacking verifiability and accountability. Misconfigurations can cause outages and instability in the system, and a non-systematic approach to configuring AutoRAN may lead to delays in troubleshooting and detecting root causes for failures.

Therefore, we introduce a RAN-Infrastructure-as-Code declarative approach for AutoRAN, as shown through the template flows in Figure 2. We define the status and configuration of the system through templates and configuration files, with key/value pairs describing how each hardware and software component of AutoRAN needs to be managed (e.g., specifying how many cores are reserved or isolated, GPU configuration). Specific examples are provided in Section IV. We implement a *GitOps* workflow to version, track, and deploy such configurations. A central `git` server hosts the template files, which include machine configurations, Dockerfiles, Helm charts, and other text-based templates. CI/CD pipelines automatically synchronize the repository on the `git` server with the hardware and services on the cluster. This guarantees that updates are automatically synchronized and aligned across production and the versioning server, and enforces a single and specific workflow to propagate changes and updates.

The CI/CD for the declarative approach is implemented through two main components, *ArgoCD* and *Tekton*. *ArgoCD* is used to synchronize configurations between the `git` server (e.g., GitHub) and the AutoRAN cluster. This also guarantees a stateless cluster, which can be deployed (or re-deployed) in few simple steps, compared to a long set of tedious manual configurations. *Tekton* is an open-source framework for designing and running CI/CD. *Tekton* pipelines consist of a declarative set of tasks executed one after the other, configured from sets of parameters passed as input. The parameters can be provided through default values as part of the pipeline definition, customized to ingest the output of other processes (as we discuss in Section V-A), or manually overridden. *Tekton* can be

accessed through APIs, making it easier to deploy applications on demand from within and outside the cluster.

C. Disaggregation, APIs, and Micro-Services

The software that constitutes AutoRAN components is deployed as a set of micro-services which are atomic—yet connected—units deployed as pods on the cluster. A pod is a set of one or more Docker containers that provide functionalities to fully express a micro-service. AutoRAN micro-services include the actual applications for the cluster, i.e., RAN, core network, RICs, and edge services, as shown at the center of Figure 2, and the software that supports the cluster and automation itself. In this sense, there exist a unified workflow and management procedures for both classes of services, simplifying the overall design of the system.

As we discuss in Section IV, a specific effort has been put into the design of the micro-services to (i) identify the degree of disaggregation that enables flexibility, automation, and scaling without compromising performance (e.g., whether different micro-services can be used for L1 and L2/L3 in a DU, or whether to split DU and CU in different pods, among others); and to (ii) separate state and logic as much as possible. The latter allows the deployment of lightweight micro-services that embed the application logic but not complex data structures, which are instead on a permanent storage layer. This provides redundancy through disk replication via Redundant Array of Independent Disks (RAID) and exposes its resources to the micro-services, or pods, so that they do not have to replicate state whenever they are deployed or perform complex operations on tear-down to store and manage the state.

The disaggregation is based on a functional split. For the 5G E2E application, it is aligned to 3rd Generation Partnership Project (3GPP) and O-RAN specifications, which include a Service Based Architecture (SBA) for the core network and a gNB split into CU and DU (software-based) and RU. Furthermore, the RICs are also deployed as set of micro-services, which can be extended by onboarding custom logic (xApps, rApps). Interfaces for cellular network components are typically defined by standards or technical specifications from 3GPP, facilitating functionality over IP networks. In contrast, services such as automation and cluster functionalities are functionally split without strict adherence to specific standards. Their interfaces are implemented via application-level endpoints or APIs, often based on frameworks like Flask. Detailed API designs for various micro-services (e.g., automated testing or intent-based deployment) are discussed in Section V.

Similarly to the infrastructure, micro-services are also defined through a declarative approach, with Helm charts defining a set of unit elements to deploy (e.g., containers in a pod, the associated storage, networking capabilities, among others) and Dockerfiles specifying the features within a specific container (e.g., what software is used to execute DU functionalities). As discussed in Section IV, we have designed an automated container build process targeting multiple architectures, as well as continuous deployment solutions, all based on Tekton pipelines.

D. Orchestration

The micro-services lifecycle is managed through an orchestrator, which takes care of handling the complexity associated to matching resources, micro-services, configurations, and cluster capabilities. The orchestrator takes care of micro-services deployment, scaling, networking, and lifecycle management, based on declarative input provided through the CI/CD approach discussed in Section III-B. Once the desired state of the system is defined (e.g., the number of replicas or specific configurations), the system continuously self-heals to maintain that state. This is done automatically, solving problems related to system complexity, ensuring high availability through automatic failover and scaling, and optimizing resource usage. The orchestrator controls operations over the infrastructure cluster, as defined in Section III-A, matching micro-services to available resources. For example, it can ensure that a DU requiring GPU acceleration is instantiated on a compute node with an available GPU and NIC.

In our setup, and as described in Section IV, we use Red Hat OpenShift, a commercial version of Kubernetes, as the orchestrator engine for our micro-services, which we tune, instrument, and configure to support the variety of 5G workloads provided by AutoRAN. Compared to other orchestration and virtualization tools, OpenShift provides superior flexibility and scalability. For instance, Ubuntu MaaS supports automated infrastructure deployment but lacks a container-based, parallel, and multi-node design. Ansible Playbooks enable automated deployments but do not offer the interactive and hybrid experimentation environment of AutoRAN. Docker-based approaches face scaling issues with technologies such as SR-IOV and Multi-Instance GPU (MIG), due to limited intent-based resource management. In general, most alternatives manage independent nodes rather than unified clusters. By contrast, Kubernetes natively supports multi-node orchestration, and OpenShift extends it with integrated automation tools like Tekton, delivering a production-ready solution.

The orchestrator also provides additional tools that can be used to manage the system. AutoRAN leverages (i) namespaces, i.e., logical partitions to organize micro-services across, for example, application domains (e.g., pods for a core network, a RIC, the RAN) or tenants (e.g., different operators sharing the same infrastructure); and (ii) advanced networking capabilities, which enable automated service discovery and the establishment of complex network overlays across micro-services (e.g., dynamically establishing routes between core network micro-services and new CUs instantiated through automation).

The orchestrator, finally, introduces a zero-touch approach into the network and system configuration, behaving as an intent-driven platform for automated deployment and testing. Although the automation capabilities of AutoRAN can enable fully autonomous zero-touch operations, in this paper we focus on their use for streamlining and automating deployments, test generation and execution.

E. High-Level Intents to Represent Network Status

While automation, CI/CD, orchestration, and declarative approaches simplify the management of a 5G network from a

system perspective, they still represent complex tools to use for a variety of end users that could be interested in managing and operating such networks. Consider, for example, private 5G deployments, where the enterprise IT team comes with limited knowledge on radio systems: expressing a rich configuration for the system components may be challenging, even if it is then automatically deployed and applied to the network. Similarly, teams with expertise on radio systems may have more limited knowledge on configuring orchestrators and micro-services.

Therefore, we design AutoRAN with a mechanism to provide high-level input for the system configuration, which is then translated into actionable templates and pipeline triggers that are automatically applied to the system. As shown in the top left part of Figure 2, users can express high-level requests to instantiate services or tests (e.g., “*deploy a 5G base station*”), which are parsed through an LLM matching the intent with templates to be applied to the system. We provide details on the implementation of this mechanism in Section V.

F. Observability

Finally, once the system is configured, deployed, and operational, the AutoRAN design also embeds procedures to automatically monitor the system status and coordinate with the orchestrator to maintain the desired system state. AutoRAN leverages Prometheus [28], OpenShift APIs, and Observium [29] to track application performance, resource consumption, and network status in real time. These tools work together to capture and visualize key metrics, e.g., CPU load, memory usage, and network traffic, and enable identification of anomalies, resource management, and continuous improvements to the overall system reliability and efficiency.

IV. AUTORAN SYSTEM COMPONENTS

The AutoRAN framework runs on a multi-architecture Red Hat OpenShift cluster capable of virtualizing and streamlining the deployment of application workloads on a generic infrastructure, which can optionally interface with specialized hardware. These workloads include RAN, core network components, RICs, dApps, xApps, and rApps, AI services and functions, as well as those that handle the automated deployment of a fully compliant 5G network managed by O-RAN. Unlike bare metal deployments, AutoRAN leverages the virtualization capabilities offered by OpenShift for enhanced flexibility and dynamic reconfiguration of the elements deployed on the 5G network.

In this section, we will describe the core components that enable the automation performed by AutoRAN. Section IV-A describes the OpenShift cluster leveraged by AutoRAN, with operators and configuration profiles detailed in Sections IV-B and IV-C, respectively. Section IV-D describes how to integrate and deploy RAN workloads using the O-RAN 7.2 split, with and without a layer-1 accelerator, and with SDRs based on a 8.1 split. Finally, Section IV-E details how to manage and build images for heterogeneous architectures, while Section IV-F reviews additional software components of the cluster.

A. The Automation Cluster

The AutoRAN architecture is depicted at a high level in Figure 3. AutoRAN is hosted in an OpenShift cluster composed of 13 nodes with heterogeneous computing hardware (summarized in Table I) and a dedicated Network Attached Storage (NAS). The backhauling and networking infrastructure leverages Software-defined Networking (SDN) switches with up to 100 Gbps connectivity and Precision Time Protocol (PTP) synchronization through a rooftop-mounted GPS antenna and local Qulsar clocks [9].

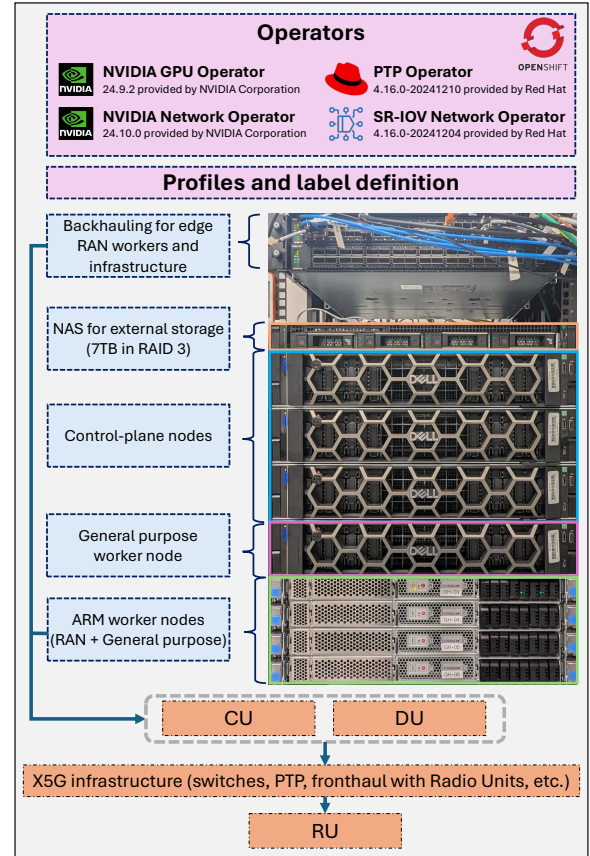


Fig. 3: An overview of the AutoRAN cluster.

Compute nodes are differentiated into control-plane and worker nodes. The former are used to host automation, control and monitoring functionalities of the cluster, as well as generic core network, RIC, and AI workloads. The latter are optimized to host RAN workloads and services via low-latency configurations and GPU acceleration capabilities. However, concurrently supporting RAN and generic cloud computing workloads comes with specific requirements on the underlying infrastructure. As detailed in Table I, we select high-performance servers with different architectures (x86 and ARM) and acceleration capabilities (e.g., the Grace Hopper MGX GH200 ARM nodes used to run the GPU-accelerated NVIDIA ARC solution) to meet the stringent RAN requirements. Key considerations also include maximizing physical CPU cores, as RAN workloads benefit from disabled hyperthreading functionalities [30], and require isolated cores for optimal performance.

TABLE I: Node architectures being integrated in the AutoRAN framework.

Model	CPU	GPU	NIC
Dell R760	Intel Xeon 8462Y+	NVIDIA L40S (40GB)	Broadcom
Microway EPYC	AMD EPYC 7262	N.A.	Mellanox ConnectX-6
Gigabyte E251	Intel Xeon 6240R	NVIDIA A100 (40/80 GB)	Mellanox ConnectX-6
Supermicro ARS-111GL-NHR	Grace CPU	NVIDIA H100 Tensor Core GPU	Mellanox ConnectX-7

Servers connect to the cluster via 10 Gbps connections to the backhaul switch, and to the fronthaul interface and RUs via dedicated 100 Gbps connections to satisfy fronthaul traffic requirements (e.g., each 4×4 MIMO RU with standard 9-bit compression requires a 10 Gbps connection). AutoRAN also consolidates multiple DUs on each node, thus calling for a 100 Gbps NIC. A PTP-compatible NIC is also needed for carrying fronthaul traffic while maintaining precise synchronization through PTP timestamping. Finally, AutoRAN also includes a persistent storage via a dedicated NAS. We separate *computing* from *storage* resources for resilience, thus obtaining a **stateless** cluster. Specifically, the NAS used by AutoRAN includes 12 TB of storage in RAID 3 using the open-source TrueNAS solution [31] to share volumes over the NFS protocol. The RAID 3 redundancy level implements a replica of the data over three separate disks, where two are used for data, while the third one is used for parity, which makes the usable disk space 8 TB.

B. Operators for Automatic Configuration

We leverage *operators* for the configuration of AutoRAN OpenShift nodes. These provide an high-level declarative approach for deterministic configuration of nodes of the cluster. The most relevant operators used in AutoRAN are summarized in Table II and detailed in the remaining of this section.

TABLE II: List of OpenShift operators.

Name	Function
Node Feature Discovery	Exports hardware and software features of nodes and label nodes
NVIDIA GPU Operator	Installs NVIDIA GPU drivers on all nodes and exposes various capabilities
NVIDIA Network Operator	Upgrades and configures NVIDIA NIC firmware
SR-IOV operator	Splits the NIC into partitions and instantiates networks
PTP operator	Provides ns clock accuracy to the pods on the node

Node Feature Discovery. Since cloud-based deployments may run on very different hardware, the Node Feature Discovery (NFD) automatically expose the features of the underlying physical infrastructure (e.g., CPU model and architecture, number of cores, amount of memory, GPU availability and type, among others) to applications and workload using labels. These labels allow the cluster to perform targeted deployments, either on a particular set of nodes or on the specific node. This ensures that components, operators, and deployments are instantiated on the nodes with the required resources.

PTP Operator. RAN systems require precise timing synchronization across their components. In general, clock synchronization is achieved through the Network Time Protocol

(NTP), which is able to provide *millisecond* accuracy over Local Area Network (LAN) setups. However, the level of accuracy delivered by NTP is not sufficient to support RAN applications, where the Open Fronthaul interface requires *nanosecond* accuracy. We therefore use PTP, a protocol that shares a synchronization signal over Ethernet, to sync all nodes and radios to a common clock source—a Qulsar clock with a GPS input in our case. The Linux implementation of the protocol uses two pieces of software, namely `ptp4l` and `phc2sys`, which are installed via the OpenShift PTP operator. The operator also gives the possibility of increasing the priority of these processes, allowing one to use them on shared CPUs rather than on a dedicated CPU per process, saving one extra core for other workloads. Listing 1 shows the PTP configuration adapted for the Grace Hopper server.

```

1 apiVersion: ptp.openshift.io/v1
2 kind: PtpConfig
3 metadata:
4   name: ptp-gh
5   namespace: openshift-ptp
6 spec:
7   profile:
8     - interface: enpls0f0np0
9       name: ptp-gh
10      phc2sysOpts: '-a -r -r -n 24'
11      ptp4lConf: |
12        [global]
13        dataset_comparison           G.8275.x
14        G.8275.defaultDS.localPriority 128
15        maxStepsRemoved             255
16        logAnnounceInterval         -3
17        logSyncInterval             -4
18        logMinDelayReqInterval      -4
19        G.8275.portDS.localPriority 128
20        network_transport           L2
21        domainNumber                24
22        tx_timestamp_timeout        30
23        slaveOnly 1
24
25        clock_servo pi
26        step_threshold 1.0
27        egressLatency 28
28        pi_proportional_const 4.65
29        pi_integral_const 0.1
30
31      [enpls0f0np0]
32        announceReceiptTimeout 3
33        delay_mechanism E2E
34        network_transport L2
35      ptpClockThreshold:
36        holdOverTimeout: 5
37        maxOffsetThreshold: 50
38        minOffsetThreshold: -50
39      ptpSchedulingPolicy: SCHED_FIFO
40      ptpSchedulingPriority: 65
41    recommend:
42      - match:
43        - nodeLabel: node-role.kubernetes.io/worker-gh
44        priority: 4
45        profile: ptp-gh

```

Listing 1: Example of a PTP profile on a Grace Hopper node.

NVIDIA Operators. These include the NVIDIA GPU Operator and the NVIDIA Network Operator. The NVIDIA GPU

Operator is in charge of installing and maintaining NVIDIA GPU drivers. GPUs are used in AutoRAN for both AI workloads (e.g., LLMs, training and testing of models) and for the NVIDIA ARC deployment [9], which uses GPUs to accelerate the DU-low operations 5G gNBs. Specifically, NVIDIA ARC requires the Open Kernel Modules instead of the proprietary drivers. We also provision GDRCopy [32] in the NVIDIA operator so that it is automatically deployed on all nodes and can directly access the GPU memory. This is a low-latency GPU memory copy library based on NVIDIA GPUDirect RDMA technology, that creates the CPU mapping of GPU memory.

The NVIDIA Network Operator is used to enable intercommunication between GPU and NIC. It is used to access the firmware of the NIC, for example, to enable higher timing accuracy and specific QoS.

SR-IOV Operator. This operator is in charge of creating virtual slices—or *virtual functions*—of the physical NIC interfaces and to expose them as objects inside OpenShift. In OpenShift and Kubernetes deployments, these are created using configuration files called SR-IOV Networks Node Attachment. After splitting the interfaces, OpenShift implements `Network` attachments to specify the IP addressing of the network and the VLAN tag. As it will be discussed in Section IV-D, NVIDIA ARC deployments require interfaces to be passed as untagged, whereas OAI requires the tag to be set on the fronthaul port. This becomes key as different deployments need different settings on the physical port, and it enables parallelization of multiple workloads on the same compute nodes. Additionally, without using SR-IOV, a NIC can only be accessed by a single container (e.g., a DU) at a time, whereas, with SR-IOV, it is possible to run multiple applications requiring access to same physical interface by connecting each of them to the virtual interfaces created by SR-IOV. This is used, for instance to parallelize multiple NVIDIA ARC deployments by running the L1 over the virtualized SR-IOV interface, where we partition each NIC into 8 virtual interfaces. For this number of partitions, we do not observe a significant increase in latency compared to bare metal or Docker-based setups. To the best of our knowledge, we are the first in following this approach with NVIDIA ARC.

An example of definition of networks over SR-IOV devices is shown in Listing 2. A `resourceName` exposes the underlying sets of virtual functions (8 in this case) created from the selected NIC. A network is then created on the virtualized NIC with parameters including VLAN tags, and IPs.

C. Configuration Profiles

Due to the stringent latency and processing requirements of RAN workloads, it is important to make sure that host machines use an appropriate kernel version and are configured to meet such requirements. This includes setting isolated CPUs, HugePages and disabling energy saving functionalities that might put the processor in an idle state and decrease performance. We use labels to automatically apply configurations to nodes upon their addition to the cluster. Nodes with the same physical hardware and configurations are grouped together in an Machine Configuration Pool (MCP). Then, for each MCP, we apply the same set of configurations.

```

1  apiVersion: sriovnetwork.openshift.io/v1
2  kind: SriovNetworkNodePolicy
3  metadata:
4    name: gh-vf-sriov
5    namespace: openshift-sriov-network-operator
6  spec:
7    resourceName: vfgh
8    nodeSelector:
9      node-role.kubernetes.io/worker-gh: ""
10   numVfs: 8
11   mtu: 9216
12   priority: 1
13   nicSelector:
14     vendor: "15b3"
15     deviceID: "a2dc"
16     rootDevices:
17       - "0000:01:00.0"
18   isRdma: true
19   needVhostNet: true
20   deviceType: netdevice
21 ---
22 apiVersion: sriovnetwork.openshift.io/v1
23 kind: SriovNetwork
24 metadata:
25   name: gh-vnf-net
26   namespace: openshift-sriov-network-operator
27 spec:
28   ipam: |
29     ## any IP address configurations, if needed
30   resourceName: vfgh
31   networkNamespace: aerial
32   # vlan: 2 # if a VLAN tag is needed

```

Listing 2: Example of a SR-IOV network policy and its network attachment.

We use `PerformanceProfile` objects to: (i) configure the number of *reserved* and *isolated* cores; (ii) enable `HugePages` to directly allocate blocks of memory (1 GB for x86 nodes, 512 MB for ARM deployments); and (iii) fine-tune kernel parameters related to interrupts and energy, e.g., disabling sleep states and offsetting the periodic clock ticks to mitigate jitter. An example of a `PerformanceProfile` for a Grace Hopper node is shown in Listing 3. In addition, different PTP profiles

```

1  apiVersion: performance.openshift.io/v2
2  kind: PerformanceProfile
3  metadata:
4    name: gh-performanceprofile
5  annotations:
6    performance.openshift.io/ignore-cgroups-version:
7      "true"
8    kubeletconfig.experimental: |
9      ## various kubelet parameters for fine-tuned
10     optimizations
11 spec:
12   additionalKernelArgs:
13     - "tsc=reliable"
14     - "nohz_full=4-64"
15     - "preempt=none"
16     - "..."
17   cpu:
18     isolated: 4-64
19     reserved: 0-3,65-71
20   hugePages:
21     defaultHugePagesSize: "512Mi"
22     pages:
23       - size: "512Mi"
24         count: 48
25   nodeSelector:
26     node-role.kubernetes.io/worker-gh: ""
27   machineConfigPoolSelector:
28     machineconfiguration.openshift.io/role: worker-gh
29   numa:
30     topologyPolicy: "none"
31   workloadHints:
32     realTime: true
33     highPowerConsumption: true

```

Listing 3: Example of performance profile for a Grace Hopper machine. are also applied to each server, taking into account their hard-

ware specifications and configuration parameters (for example, the name of the specific network interface that should receive the synchronization signal).

Profiles linked to a label are immediately applied to each new labeled node. Nodes update in a rolling strategy and, at the end of the update, their configurations are aligned, which eliminates the risk of stale drivers. This flexibility in node labeling and zero-touch configuration is even more relevant for extendability and scalability of the framework. Indeed, multiple profiles can be prepared in advance and applied to MCPs. If a node—or a set of nodes—needs to be adapted for different workloads (from RAN to generic cloud computing or high-performance computing), it is only necessary to relabel the node so as to make it part of a different MCP with different configurations, and the node gets automatically provisioned.

Finally, it is worth mentioning that differently from bare-metal or Kubernetes-based deployments, OpenShift only supports generic or real-time kernels (from no other sources than Red Hat itself), and does not support the low-latency ones generally recommended for gNB protocol stacks. Since at this time the NVIDIA L1 deployment requires drivers that are not available for Red Hat’s real-time kernel, we adopt the generic Linux kernel on all the cluster nodes. Experimental evidence in [14] also shows the instabilities of real-time kernels for RAN deployments, which results in poorer performance when compared to the generic one.

D. Integrating RAN Deployments

We validated a set of deployments that can be instantiated on the AutoRAN infrastructure at this time. These deployments, shown in Table III, include deployments with both commercial radios with support for the O-RAN 7.2 split, SDR (e.g., Universal Software Radio Peripherals (USRPs)), as well as CPU- and GPU-accelerated DU solutions. We extend the USRP-

TABLE III: Protocol stack and OTA RU pairs validated on AutoRAN.

gNB stack	Fronthaul/L1	RUs
NVIDIA ARC	GPU Acc. L1	Foxconn RPQN (100 MHz)
OAI	OSC FH	Foxconn RPQN (20/40/100 MHz)
OAI	N/A	USRP x310/x410
srsRAN	N/A	USRP x310/x410

based deployment proposed in [14], [13]. Pods are assigned one SR-IOV device, whose physical NIC is connected through a switch to the USRPs deployed in our laboratory environment. This kind of deployment resembles the O-RAN 8.1 split, since the entire logic of the disaggregated gNB is focused on the CU/DU. We, then, proceed to include the O-RAN 7.2 split-based deployments, focusing in particular on OAI and NVIDIA ARC. This split divides the functionalities of a traditional Base Band Unit (BBU) into two parts: high-PHY processing remains in the DU, while low-PHY processing is moved to the RU. This enables effective centralization of compute resources in the DU, while the RU can be simplified and deployed closer to the antennas. It also supports robust signal processing capabilities and reduces latency by minimizing the fronthaul bandwidth requirements between DU and RU.

To support the 7.2 split, it is necessary to use high-performance and low-latency compute nodes that can sustain the high processing requirements of the Open Fronthaul and the low-DU. OAI integrates an OSC library that provides support for the 7.2 split, while ARC uses an NVIDIA library for x86 and ARM architectures.¹ Moreover, both the OpenAirInterface and NVIDIA ARC platforms require Data Plane Development Kit (DPDK), a set of libraries that accelerate the processing of packets to support real-time operations. For the 7.2 OAI deployment, we deploy a single pod containing OAI gNB, which requires two tagged SR-IOV devices, one for the control plane and one for the user plane, each accelerated by DPDK.

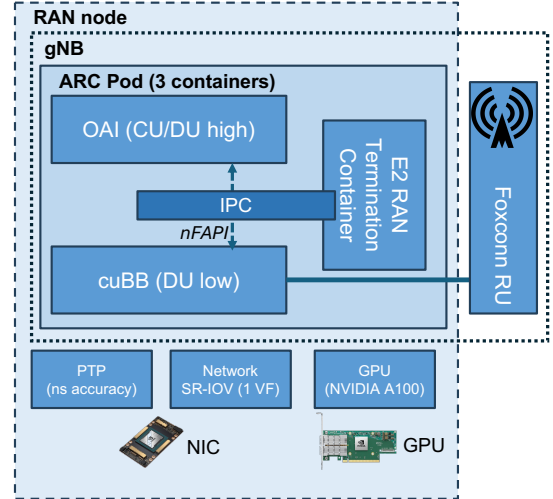


Fig. 4: ARC deployment in AutoRAN.

Differently, the NVIDIA ARC setup requires a more complex deployment. Specifically, NVIDIA ARC usually runs as a combination of two containers, one for the L1 accelerator, called cuBB, and the other one for the L2, based on OAI. The communication between L1 and L2 happens via Inter-process Communication (IPC) shared between the two containers. The original implementation from NVIDIA is based on Docker containers that access directly the NIC and the hardware using the Host Network Mode, that is without any layer of networking virtualization. Differently from this approach, we remove the host network requirement and we run NVIDIA ARC over virtualized NICs using an untagged port since the L1 is in charge of adding the VLAN tag. In OpenShift and Kubernetes, this can be achieved either via two pods, each with a single container, or a single pod with two containers. We choose the latter deployment option (shown in Figure 4, where we also add the E2 termination described in [9]) to support the instantiation of multiple NVIDIA ARC containers (e.g., to deploy multiple gNBs) because both L1 and L2 are tightly coupled, and requires shared memory and networking.

All gNBs based on the 7.2 split and without GPU accelerator share the same deployment structure. Therefore, when a new radio—real or emulated as RuSIM—gets integrated into AutoRAN, the only modification required is in the template of

¹It is worth recalling that NVIDIA ARC also uses OAI for the DU-high and CU.

the configuration file. The same applies, for both L1 and L2 configuration files, to the NVIDIA ARC deployment.

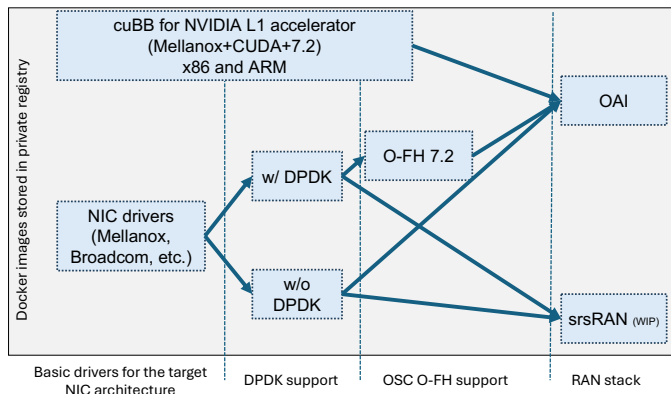


Fig. 5: Chained building procedure.

E. Container Image Building

Another important aspect for a virtualized deployment is the building of container images. Unlike cloud computing use cases, where images are generic, RAN deployments require instruction sets optimized for the specific CPU architecture and host family where the container will be instantiated. A possible approach is to build the image for a specific architecture by specifying flags to the Dockerfiles (e.g., a *cascadelake* architecture flag). This makes it possible to build images on any node in the cluster. However, it requires different Dockerfiles for different deployment. Another approach, which is the one we follow, consists in building the image on the target deployment node (e.g., if we want to run OAI on a Grace Hopper node, we build the image on a Grace Hopper directly). In this way, we build images for each node without the need for different Dockerfiles. As we will show later in Section VI-E, thanks to the isolation between cores and processes, the build process does not affect the performance of the RAN.

To maximize image reuse and reduce build times, images are built in a chained manner, as shown in Figure 5. Specifically, different gNB images (e.g., OAI, srsRAN) and their subsequent versions (e.g., among different weekly tags in the case of OAI) might share common dependencies, e.g., in terms of NIC drivers, DPDK, etc. Instead of rebuilding all the dependencies for each new image, we maintain dedicated images with the required dependencies installed but no gNB software. We, then, use these images as a base to build the gNB images, thus speeding up the build process at the cost of additional images (i.e., the dependencies images) stored on the registry. Since AutoRAN is deployed across heterogeneous server architectures (ARM and x86) and CPU models (e.g., Cascade Lake, Sapphire Rapids), we adopt an MCP-specific build approach. To ensure that each RAN image fully leverages the capabilities of the hosting node, images are built directly on the nodes where the corresponding workloads will be executed.

F. Additional Software Components

In addition to the RAN workloads, a fully operational Open RAN requires several other elements. The core network is

in charge of operations such as user authentication and the creation of Packet Data Unit (PDU) sessions. Among the various core networks available in the literature, we deployed Open5GS. However, AutoRAN is not bound to a specific core network, and we decided to focus on Open5GS due to its high performance and ease of installations in Kubernetes-based deployments, where we deploy multiple independent replicas with different PLMNs for different tenants.

Another key element of an O-RAN deployment is the RIC, a component that enables observability and control of the network [33]. Specifically, Near-Real-Time (Near-RT) control is achieved via applications called xApps deployed on the Near-RT RIC, while Non-RT control via rApps deployed on the Non-RT RIC. We deploy an OSC Near-RT RIC (“E” release) and connect it to OAI via the E2 agent provided in [9], [34] and publicly available as part of the OpenRAN Gym framework [35]. Finally, the cluster also hosts a non-RT RIC to enable observability at larger time scales.

V. AUTORAN END-TO-END WORKFLOWS

In this section, we focus on providing details on how to leverage such blocks to automate the deployment, management and testing of a private 5G network Over-The-Air (OTA). Specifically, we extend our previous work [14] to support a broader set of testing operations and technologies, deploy and test automatically different combinations of protocol stacks and RUs (see Table III) in a repeatable manner, and analyze their performance under different conditions (e.g. number of users, target data rate, and arbitrary protocol configuration files). As we describe later, this is done through a set of pipelines that process high-level, user-specified requirements regarding the specific configuration to test (e.g. OAI with a certain RU and MIMO configuration) and convert them into deployment and testing operations. These involve (i) instantiation of the 5G software containers as pods; (ii) initialization and attachment of UEs; and (iii) data collection of relevant performance metrics to evaluate test success. Additionally, such deployment and testing configurations can be automatically generated through LLMs starting from a high-level intent, and then actuated by the above pipelines, as discussed in Section V-A. To streamline and automate testing procedures and support remote execution of tests, our UEs are Sierra Wireless EM9191 5G modems connected to mini-PCs (e.g., Intel NUC, or Raspberry Pi). The UEs’s mini-PCs are used as host machines that pilot the UE to perform attachment operations via AT commands embedded in the Qualcomm’s chipset, generate traffic and collect data.

AutoRAN Workflows. The workflows for the deployment and testing of Open RAN components are shown in Figure 6. The blue blocks in the figure concern the instantiation of workload, while the pink ones carry out the functionalities related to testing. The deployment workflow involves steps from the creation of generic deployment specifications, to their specialization to the hardware infrastructure and available resources. Similarly, the test workflow concerns the creation of generic test specifications, their specialization to the testing infrastructure, the actual test execution, and data collection and analysis. The steps for both deployment and testing workflows will be detailed in the remaining Sections V-B and V-C respectively.

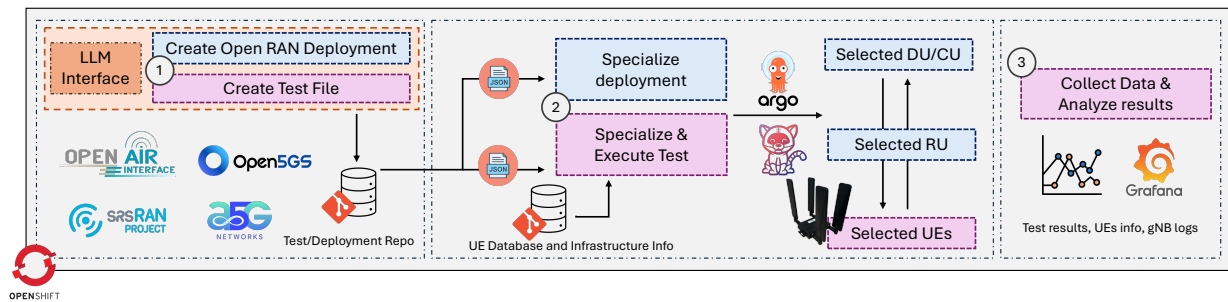


Fig. 6: E2E automated testing diagram.

A. Intent-based Instantiation and Testing

In the following paragraphs, we describe how we leverage AutoRAN to simplify and streamline network instantiation procedures and testing via intent-based deployment and testing, leveraging natural language processing. The goal of this feature is to eliminate complexity related to network configuration and allow even non-expert users to deploy and test a full-fledged network using only Natural Language (NL). Examples of possible intents include queries such as “*deploy a 5G gNB with OAI and NVIDIA Aerial Research Cloud (ARC)*” or “*perform a 15 Mbps iPerf test with 3 UEs*”. In order to process NL, we opt for using LLMs as they provide capabilities to parse text, understand context and need, and convert them into structured and machine-understandable directives. Given the large availability of pre-trained models with excellent performance for a variety of tasks under different benchmarks, we opt for using a pre-trained LLM (Qwen 2.5) in an agentic setup, i.e., where the LLM makes calls to a set of tools (defined thereafter) in iterative loops.

Although appealing for their simplicity, LLMs are also well known for sometimes drifting away from initial instructions and producing hallucinations. In our case, this is particularly relevant, as any hallucination could result in incorrect network configuration that might produce wrong/misleading test results and even generate outages. To prevent this unwanted behavior, we design a set of procedures (depicted in Figure 7) that constrain the output of the LLM, forcing it to output the correct network/test configurations.

Achieving this in practice is not trivial, and presents several challenges:

- First, it should be noted that not all the RAN components available in AutoRAN are compatible with each other. For example, OAI supports the ARC L1, while srsRAN does not, meaning we need to prevent the LLM from trying to configure a srsRAN base station with ARC, which would result in a non-working deployment. It is therefore fundamental to ensure that the LLM only selects compatible components and configurations (e.g., OAI with ARC, plain OAI/srsRAN, as shown in Table III). For this reason, we store a compatibility graph, indicating which network components (DU, CU, RU, Core Network) are compatible with one another. Similarly, for each test type, a graph of the list of compatible parameters is fed to the LLM (for example, tests using different traffic generators, such as Multi-Generator (MGEN) can include parameters such as the distribution of traffic, while iPerf tests do not). In the workflow of Figure 7, the compatibility

graph is used in the process to validate the configurations generated by the LLM by making sure that those include elements that are compatible with one another. When a new technology (CU, DU, RU) becomes available and integrated, the dependability graph is updated to reflect the compatibility between that specific element and the others available in AutoRAN.

- Second, the LLM might output some text that drifts slightly from the anticipated output, causing potential parsing issues and undefined behaviors, such as outputting incorrect attribute values. We solve this issue by using the tool-calling feature of recent LLMs. With this feature, we can feed the LLM with a list of tools which it can explicitly call by outputting special tokens. In our case, those tools consist of a set of pre-defined Python functions which (i) set the values of the network parameters in a dictionary (e.g., associate each possible parameter such as CU/DU/RU) with a value (in Figure 7, this corresponds to the update of parameters); and (ii) verify that the set values are correct, i.e., that they correspond to valid parameters which are compatible with one another (in the value validation step).
- Another issue is that while most LLMs can follow instructions, the complexity of the network configuration task calls for multiple long instructions (this includes describing the use-case, the infrastructure, the compatibility graph, etc.). The result is that most models manage to follow some of the instructions, but rarely all of them at the same time. For this reason, instead of relying on a single prompting round, as shown in Figure 7, we resort to a looping mechanism in which the LLM is fed back with reports on misconfigurations and missing configuration fields. This enables the LLM to build the requested configuration iteratively, in a two phase manner where it first loops until all parameters have been populated with a correct value. Then, in the second phase, the validity is verified by ensuring that the configuration matches the compatibility graph.

Once we obtain the correct configuration (i.e., when there is no more error message in Figure 7), we convert it into json format and send it to the correct pipeline (either the testing pipeline or the deployment pipeline) for execution on the cluster. This process is essential as it ensures we map intents to actionable network deployments, making sure that the selected software and hardware elements can interact with each other and can effectively deliver network services to users.

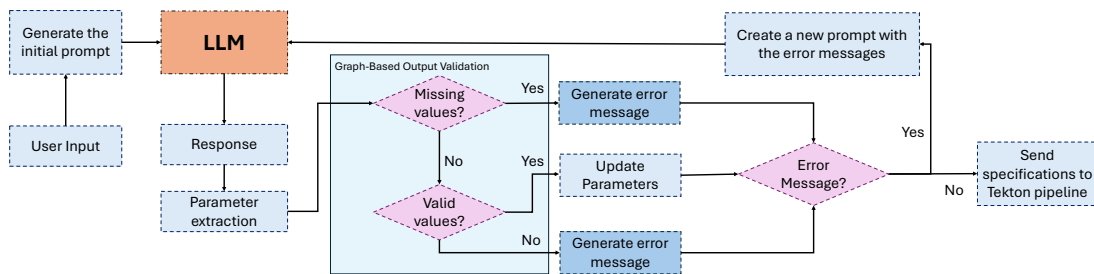


Fig. 7: LLM agent for configuration extraction.

B. Deployment Workflow

The deployment workflow is in charge of automatically instantiating the specified workloads (e.g., OAI gNB, core network, RIC) on the virtualized infrastructure. The main steps of this workflow, shown with blue boxes in Figure 6, involve: (1) creating the Open RAN deployment file; and (2) specializing this to the specific hardware infrastructure abstracted by OpenShift (e.g., selecting specific CUs/DUs and RUs). The deployment file is used to specify the workloads to instantiate on the physical infrastructure, e.g., an OAI CU/DU with Foxconn RU (see Table III for the list of possible combinations). An example of this file (and possible output of the LLM) is shown in Listing 4, where the core network (marked as `core_network` in the listing) is set to Open5GS, the protocol stack to OAI for CU/DU-high (`cu` and `du-high`) with NVIDIA ARC for DU-low (`du-low`), and RU to Foxconn (`ru`).

```

1 {
2   "network_scenario": {
3     "id": 1,
4     "core_network": {
5       "name": "open5gs"
6     },
7     "cu": {
8       "name": "oai",
9       "config_file": "oai_100_3750_2x2.conf"
10    },
11    "du-high": {
12      "name": "oai",
13      "config_file": null
14    },
15    "du-low": {
16      "name": "cubb",
17      "config_file": "cubb_100_2x2.yaml"
18    },
19    "ru": {
20      "name": "foxconn",
21      "location": 660,
22      "config_file": null
23    }
24  }
25 }

```

Listing 4: Example deployment file with the components and configurations to be tested.

After building the deployment file, we leverage Tekton pipelines to specialize the parameters therein to specific infrastructure components (e.g., the selected `ru` is converted in the MAC address of the RU), and to execute the actual deployment of the virtualized components. This is done via pipelines synchronized on the OpenShift cluster via the ArgoCD framework from a version-controlled git repository (see Section III).

Each pipeline consists of multiple *tasks* that need to be executed to successfully run the pipeline. These tasks are associated to operations that span from sending the intent of the user to the LLM, to converting the output of the latter into a

deployment object specialized to the physical infrastructure, to configuring and instantiating the gNB components (e.g., CUs and DUs) and connecting them to the radio devices used for the test (e.g., either USRP SDRs or commercial RUs) and to the core network. After instantiating the specified components in the form of virtualized containers, the gNB software is started via a call to Flask APIs that they expose. For NVIDIA-ARC deployments, the AutoRAN framework performs a single API call to start the workload. Specifically, an API endpoint is exposed by the CU/DU container. This, then, applies the correct configuration for the deployment and, using an internal connection, starts the DU-low container. Thus, by leveraging OpenShift's built-in virtualization and parallelization capabilities, AutoRAN can execute multiple experiments concurrently, provided sufficient hardware resources are available and there is no interference between the gNBs.

C. Testing Workflow

The testing workflow is in charge of automatically executing performance tests leveraging the components instantiated by the deployment workflow (see Section V-B). Its main steps, shown in pink boxes in Figure 6, concern: (1) creating a test file; (2) specializing it to the components under testing and running the actual test; and (3) collecting and analyzing test data. The test file, an example of which is shown in Listing 5, specifies various parameters for each UE, such as the network slice the UE is assigned to, the type of test to run (e.g., iPerf, MGEN), target data rate, and test duration.

```

1 {
2   "network_scenario": {
3     "id": 1,
4     "ue_specification": [
5       {
6         "slice_id": 1,
7         "test_type": "iperf",
8         "bandwidth_mbps": 25,
9         "duration": 60,
10        "protocol": "udp",
11        "reverse": true,
12        "json_output": true,
13        "server_hostname":
14          "http://server.automation.otic.open6g.net",
15        "server_port": 32201
16      }
17    ]
18  }

```

Listing 5: Example of iPerf downlink test file.

The created test file is then fed to a Tekton pipeline, which activates the specified UEs for them to connect to the deployed components (see Section V-B). Information on UEs and their

functionalities is stored in a *UE database*, an example of which is shown in Listing 6. For each UE, this database—

```

1 {
2   "btdn0140013c": {
3     "ue_hostname": "cicd-001",
4     "ue_imsi": "001010000010666",
5     "ue_ip_address": "10.112.1.53",
6     "ue_location": "660/3",
7     "ue_model": "NUC7i7DNKE",
8     "ue_serial_number": "btdn0140013c"
9   },
10  "782452cbd384d676": {
11    "ue_hostname": "cicd-002",
12    "ue_imsi": "001010000012247",
13    "ue_ip_address": "10.112.1.54",
14    "ue_location": "660/4",
15    "ue_model": "Raspberry Pi 5 Model B Rev 1.0",
16    "ue_serial_number": "782452cbd384d676"
17  },
18  "mj06k2su": {
19    "ue_hostname": "cicd-003",
20    "ue_imsi": "001010000012252",
21    "ue_ip_address": "10.112.1.52",
22    "ue_location": "640/2",
23    "ue_model": "10MUS30601",
24    "ue_serial_number": "mj06k2su"
25  }
26 }

```

Listing 6: UE database example.

automatically updated by the UEs via cron jobs—records information such as UE hostname, International Mobile Subscriber Identity (IMSI), IP address, location, and model and serial number of the mini-PC controlling the Sierra Wireless 5G modem. This automation enables continuous scalability of the system without requiring manual updates to the testing framework or UE database. Finally, once UEs are connected to the gNB, the specified traffic will start (for instance using tools such as iPerf), and results of the test will be collected and analyzed. In our tests, we deploy multiple iPerf servers to generate the traffic that the UEs request during the test, and each instance is deployed as a pod. Specific parameters of the test, such as server hostname and port, can be specified in the test files. After the specified tests have been executed, performance metrics are extracted and stored in an InfluxDB database—together with test and protocol stack logs—and visualized via a Grafana dashboard, which also lets users compare the latest test results to historical data. This, together with the automated update of the gNB protocol stack is key for observing how new releases of the protocol stack software affect the network performance, enabling users to quickly spot degradations with respect to previous tests.

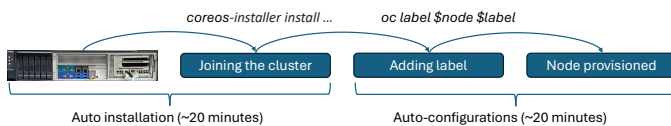


Fig. 8: Steps required to provision a new node.

VI. EXPERIMENTAL EVALUATION

The section discusses several results that profile the performance and effectiveness of the proposed AutoRAN approach. Specifically, in Section VI-A we review the time needed to onboard a new node in the cluster, comparing automation and manual solutions. In Section VI-B we describe the LLM deployment and report related metrics. In Section VI-C, we

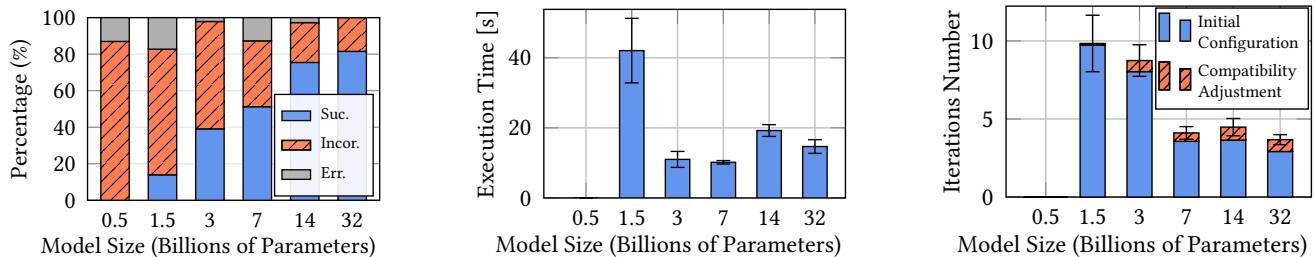
analyze the time needed to execute deployment and testing workflows using AutoRAN, showing how a network based on microservices can be instantiated in a matter of seconds. In Section VI-D, we provide performance metrics obtained from the deployed gNBs. In Section VI-E we analyze coexistence between RAN and other generic workloads. Finally, in Section VI-F, we provide insights on AutoRAN’s resiliency.

A. Onboarding Nodes on the AutoRAN Cluster

AutoRAN is designed to ensure scalability. Even the extension of the cluster follows the same principle. To showcase the benefits of automated node creation and configuration, in this section we provide a comparison between adding a new RAN worker node manually and using AutoRAN. Manually deploying a NVIDIA ARC node requires performing several error-prone steps that need to be repeated on each compute node of the cluster just to set up the basic infrastructure. This usually requires additional effort to maintain the node with up-to-date drivers and software. Using the profiles and configurations offered by AutoRAN, extending the cluster with an already configured profile requires minimal human intervention, as shown in Figure 8 (i.e., it is only required to add the node to the cluster—using `coreos-installer`—and assign a label to it—using `oc label`), and guarantees a completely configured node ready to accept any targeted workload in approximately 40 minutes—without the same level of effort of manually configuring a node. After their initial provisioning, nodes can be repurposed for different roles (e.g., edge vs RAN node) by modifying their labels. After this operation, nodes will reboot and auto-configure themselves as required.

B. LLM-Based Deployment

In this section, we evaluate our LLM-based deployment pipeline. To do so, we use Claude 3.7 Sonnet to generate a series of 33 different deployment prompts. Each prompt provides some specific requirements in NL and is associated with the required element(s) in the deployed network. For example, if the prompt is “*generate a 5G network based on GPU acceleration*”, the associated requirement is that the DU-low uses ARC. We evaluate the deployment pipeline by running each prompt 10 times, for different sizes of LLMs. The LLM is deployed on one of the control-plane nodes, which are equipped with a NVIDIA L40S GPU with 40 GB of VRAM. Figure 9a shows that the larger model is significantly better at providing satisfactory configurations, with Qwen2.5:32B reaching up to 80% correct responses, and with correctness consistently decreasing as we decrease the size of the model. Furthermore, Figure 9b shows that this extra performance does not necessarily come at the cost of a larger execution time (measured from the time the user sends the prompt to the time the input to the Tekton pipeline is generated, see Fig. 7), with Qwen2.5:1.5B having the largest runtime despite its low success-rate. We observe (see Figure 9c) that this concurs with the high number of iterations in the initial phase (where we verify if values are missing, see Figure 7): the model struggles to find any valid configuration until it times out. On the other hand, larger models have similar iteration counts due to their ability to output a correct configuration (in the sense that we almost always obtain a deployable



(a) Success rate of deployments through LLM for different sizes of Qwen2.5 LLM. (b) Runtime of LLM for successful deployments with different sizes of Qwen2.5 LLM. (c) Number of iterations for successful deployments with different sizes of Qwen2.5 LLM.

Fig. 9: Performance metrics for different sizes of Qwen2.5 LLM: (a) success rate, (b) runtime for successful deployments, and (c) number of iterations required.

network, but that network is not necessarily the one the user asked for, as per Figure 9c).

C. End-to-End Deployment and Testing Workflows

In this section, we show experimental results to validate the automated E2E test workflows described in Section V, where we use Sierra Wireless 5G modems as UEs. We leave the extension of the automated tests to smartphone UEs for future work, while we use these devices for manual and mobile tests. Figure 10 shows the time required to execute the different tasks of the automated testing pipeline discussed in Section V. To-

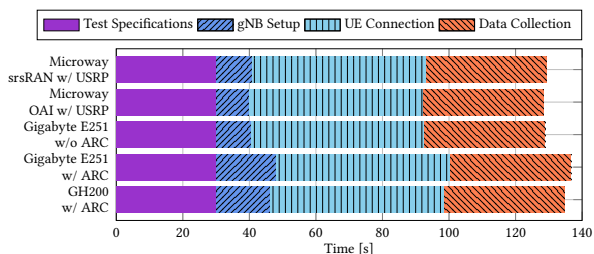


Fig. 10: Average time duration of different tasks of the automated tests. Together, the following five bars show the average time required to perform a complete test with five different gNB combinations: (i) GH200 server with ARC; (ii) Gigabyte E251 server with ARC; (iii) Gigabyte E251 server without ARC; (iv) Microway server with OAI and USRP; and (v) Microway server with srsRAN and USRP. The *Test Specification* bar shows the time taken from when the user specifies which deployment and test configuration to use, to when the gNB Flask API is called to start the test. The pull time, included in this value, is dependent on the size of the image and the network speed. Having a local and private registry inside OpenShift allows AutoRAN to pull the image at the maximum speed allowed by the connection between the cluster and the NAS, that is up to 10 Gbps. Extra time is still required to the various layers of the image in the target node. On the other hand, after the image has been pulled at least once on a node, it is thereafter kept in its cache registry, and subsequent pulls are in the order of a few milliseconds. Therefore, by pre-loading the image in the internal cache on the node, the pull time becomes negligible even for the bigger images, such as cuBB (around 40 GB). After the image has been deployed in a pod on the targeted node, the gNB software needs to be instantiated (*gNB setup* in Figure 10). As shown, the time to run the gNB on the GH200 and Gigabyte servers is

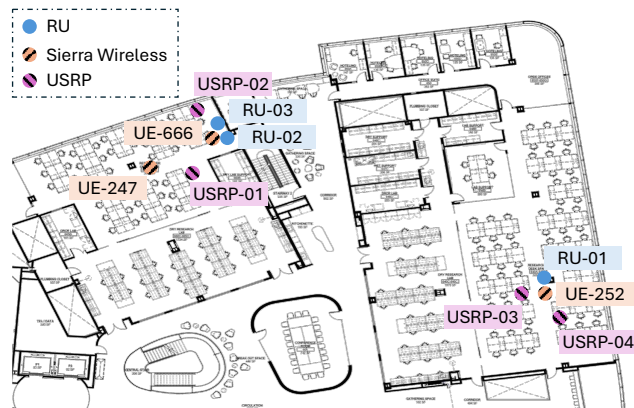


Fig. 11: Location of RUs, Sierra Wireless UEs, and USRPs used in our tests.

quite similar, at around 18 s. This time accounts for the time to initialize libraries, GPU and NIC for the L1 acceleration. On the other hand, since running OAI without ARC on the Gigabyte server only one container is needed and the gNB is monolithic, the start time is shorter, about 8 s. As the RUs are always in idle state (i.e., in the on state but without actively transmitting or receiving) and initialized outside of OpenShift via M-plane-like functionalities before the gNB pod deployment (see Section IV), we do not include initialization (approximately 60 s for a Foxconn RU) and reconfiguration times in the instantiation time of CU/DU. This is different from the USRPs deployment, where initialization times are negligible. Indeed, the time taken to start the gNB and connect it to the USRP for both srsRAN and OAI is around 10 s. Finally, the last two bars show the time taken for the UE (Sierra Wireless 5G modem in our case) to connect to the gNB, and the time taken to collect the results and send them to the data collector pod respectively. It is worth mentioning that we do not report the duration of the data transmissions between gNB and UE, as it depends on the value in the test specifications (e.g., run an iPerf test for 60 s, see Listing 5). Finally, multiple tests can be executed either as independent tests (e.g., one for iPerf with TCP and one for iPerf3 in UDP) where the gNB is restarted prior to the execution of the next test, or consecutively without redeploying the pod.

D. Performance Evaluation of RAN Functions

We show results on the performance of the RAN stacks obtained using the AutoRAN framework. In more detail, in Section VI-D1, we show metrics obtained through the automated testing of the Sierra Wireless modems deployed in static location. In Section VI-D2, we provide a comparison of the raw

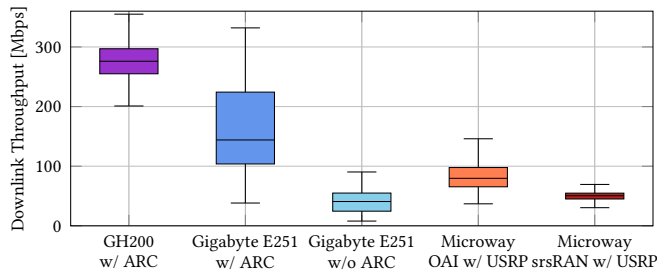


Fig. 12: Bar plot of achieved TCP downlink datarate of Sierra 5G modem with five different configurations.

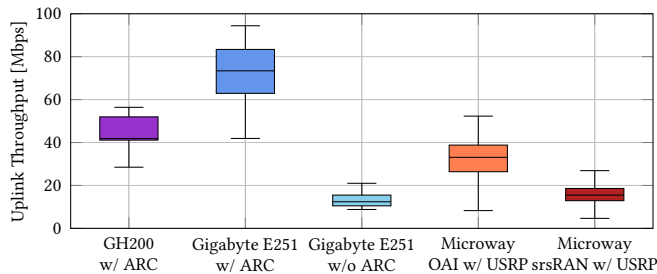


Fig. 13: Bar plot of achieved TCP uplink datarate of Sierra 5G modem with five different configurations.

performance of the L1 accelerator from NVIDIA between the original NVIDIA ARC deployment and AutoRAN's.

For over-the-air tests, the locations of the RUs and UEs used in this test within our laboratory are shown in Figure 11. Specifically, we used UE 252 and Foxconn RU-03. For the experiments with the USRPs, the USRP antennas are chosen to be at the same distance from the UE as that between UE and RU in the experiments with the Foxconn radio.

1) *Performance of the Automated Testing Workflow:* Figures 12 and 13 show the downlink and uplink TCP throughput achieved during the specific E2E experiments performed through the workflows described in Section V to test five different combinations of gNBs with a single Sierra Wireless as the UE. For this specific test, we select TCP as a way to measure not only raw performance but also the realistic goodput reaching the considered UE.

We notice that in the downlink direction, the gNB deployed with ARC on the GH200 server achieves an average throughput of 275 Mbps, which surpasses the throughput of both the ARC gNB deployed on the Gigabyte server and that of the deployments without ARC. These experiments also show that OAI achieves slightly better performance than srsRAN when they are both deployed on the Microway server and use USRP SDRs over a 60 MHz bandwidth. Uplink performance with the Sierra Wireless modem, instead, reaches more than 75 Mbps when using the ARC setup on the Gigabyte server, which outperforms the four other gNB configurations.

2) *Performance Comparison of NVIDIA ARC:* In this section, we focus on comparing, for the first time, an OpenShift-based deployment of NVIDIA ARC with its counterpart based on bare-metal and Docker virtualization. In the following, the performance we report is obtained from the cuBB L1 accelerator logs (and not from the UE), since we are interested in comparing the raw throughput being pushed by the accelerator, also considering the partitioned NIC and the extra levels of vir-

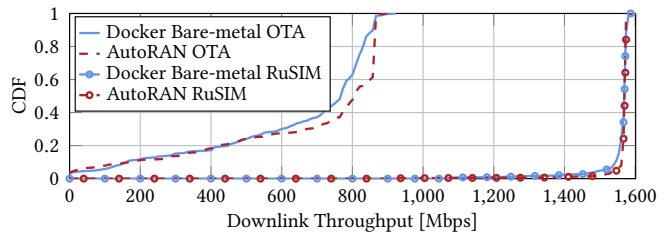


Fig. 14: Downlink comparison of OTA and RuSIM transmissions between using AutoRAN and Docker on bare metal on the Grace Hopper.

tualization. We run a comparison using OTA transmissions with a smartphone and the RuSIM emulator. Results of both experiments are shown in Figure 14. For the former configuration, we generate downlink traffic toward a single Samsung S23 phone UE in an OTA transmission using a Foxconn RU in the N78 band configured at 100 MHz bandwidth with DDDDDDSUUU as Time Division Duplexing (TDD) pattern. We test iperf3 connectivity between the phone and a server pushing 1 Gbps to the phone itself for a duration of 60 s. The Cumulative Distribution Function (CDF) is calculated as average of 5 experiments. Note that, compared to the Sierra Wireless boards used in the previous tests, this device supports 4 layers in downlink, resulting in higher achievable throughput. The results, indeed, show that the throughput in downlink reaches up to 820 Mbps, with similar performance for the AutoRAN and bare metal configuration.

To exclude any variability related to the radio environment, we also perform an emulated comparison using RuSIM, one of the Keysight tools available in the Northeastern University OTIC [36]. RuSIM is a RU emulator for 7.2 split, mirroring all parameters that a real RU should expose. In addition to this, it allows simulation of users and of wireless channel. It is usually used jointly with other Keysight tools, including CoreSIM (to emulate core network and traffic generation) and Air Mosaic for managing and orchestrating tests. AutoRAN provides a flexible testing platform and the integration of RuSIM only requires the addition of a second SR-IOV interface to communicate with CoreSIM, since it is external to the cluster. This shows the flexibility of the AutoRAN virtualization capability, since the same physical interface is used twice, for fronthaul and backhaul, using two different virtual functions. We test performance of 15 simulated users, which are able to achieve an aggregate performance of around 1600 Mbps using all slots (1600) every second available over 100 MHz with a DDDDDDSUUU TDD pattern.

Our results show that the added virtualization and integration into AutoRAN does not lead to relevant performance difference in raw throughput when deploying NVIDIA ARC gNBs. It is worth mentioning that the cuBB logs show some delayed slots from time to time in the OpenShift-based implementation (probably due to the missing optimized kernel), but this situation does not seem to affect performance. Therefore, the AutoRAN approach shows how it is possible to apply infrastructure sharing to the RAN world as in the cloud computing one without significant performance degradations.

As at the time of this writing, open-source RAN stacks are not optimized for Ultra Reliable and Low Latency Communi-

cations (URLLC) use cases, we evaluate latency by exchanging ICMP packets between a Samsung Galaxy S23 Commercial Off-the-Shelf (COTS) UE and core network on AutoRAN as well as on the bare-metal NVIDIA ARC deployment. Results for this evaluation are shown in Figure 15. We notice that the performance between the original NVIDIA ARC and the AutoRAN deployments are similar, with small variations in latency related to non-deterministic channel conditions and an average ICMP Round Trip Time (RTT) of 18 ms.

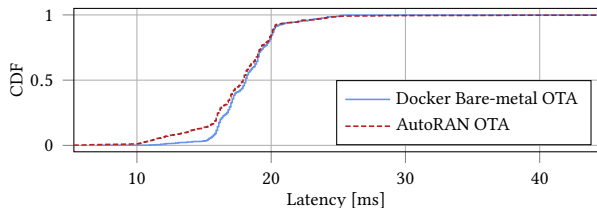


Fig. 15: CDF plot of achieved ICMP latency of a COTS UE.

E. Coexistence with Different Workloads

In this section, we test whether generic workloads on a RAN oriented node has any effect on the RAN itself. We want to evaluate this coexistence capabilities for various reasons, including building of containers on the targeted node and any other workloads that the OpenShift scheduler allocates on that node itself on the shared CPUs. We show how running increased CPU-based consumption for a long period of time does not affect the throughput of the L1. We use the RuSIM emulation in Figure 16. We simulate high demanding workloads using the Linux tool `stress` on either 10, 20, 30 isolated CPUs and on the generally available shared CPUs of the system.

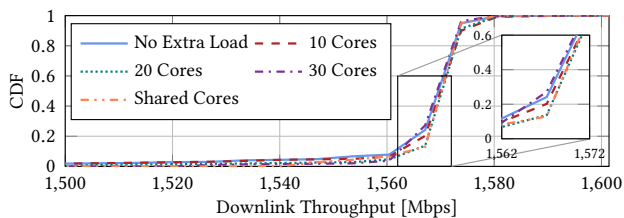


Fig. 16: Performance comparison when applying load on either N isolated and shared cores using RuSIM at full capacity.

In Figure 17, we show the coexistence of multiple RANs on the same node using the SR-IOV and MIG partitioning technologies on the Grace Hopper node. In this experiment, we consider two cells at 100 MHz: one based on RuSIM, and the other OTA with one COTS UE attached. The L1s of both RANs are completely independent in CPUs, memory, and GPU. We show that the throughput of the first active cell is not impacted by the activation of the second cell, despite sharing the same GPU. Latency is not affected by the coexistence of multiple gNBs, with the same average results as shown in Figure 15. This set of experiments shows how AutoRAN does not introduce relevant delays or performance degradation into the gNB stack while using an additional layer of virtualization and exposing a new set of features that streamlines and simplifies 5G lifecycle management.

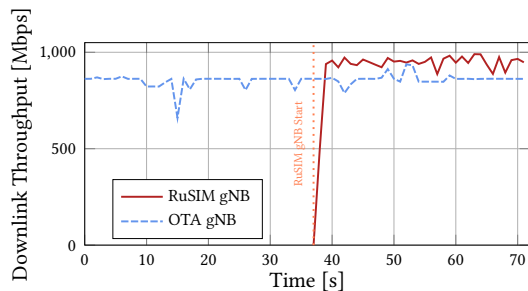


Fig. 17: Performance comparison with concurrent RAN workloads using NVIDIA ARC.

F. AutoRAN Resilience

The OpenShift container orchestration platform AutoRAN is based upon—which is, in turn, based on Kubernetes—natively provides high-availability mechanisms to compensate for node failures by “evicting” (i.e., moving) workloads from unresponsive to functioning cluster nodes. As mentioned in Section III, however, RAN workloads typically require specific hardware functionalities to be available on the compute nodes. Therefore, they can only move across nodes where these are available (in practice, across nodes part of the same MCP), while an AutoRAN-orchestrated redeployment is needed across nodes with different MCPs. The eviction happens automatically after a timeout that starts when OpenShift detects the node to be unavailable. The duration of the timeout is configurable between 0 s (the pod gets evicted as soon as the node appears unhealthy) and infinite (the pod never gets evicted), with a default of 5 minutes. Further analysis of this parameter is left for future work. Additionally, due to limitations of the protocol stack implementations we leverage, a new instantiation of the pipeline is required to re-start the gNB once the workload is re-allocated.

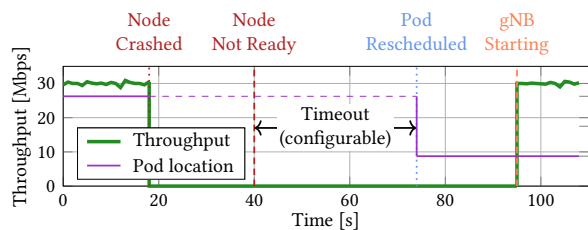


Fig. 18: Workflow of AutoRAN when a node is detected to be unavailable.

Figure 18 shows an experiment where the OpenShift scheduler detects a failed node (Microway) in around 40 s. Once this happens, OpenShift enforces a timeout (set at 30 s), after which the pod is up again and ready to start a new transmission or deployment in a new node of the same MCP. The UE, generating around 30 Mbps of traffic, gets disconnected, but it reconnects and is able to generate traffic again around 30 s after the gNB has been redeployed, similarly to what described in Figure 10. Note that, during this process, UEs can detect a Radio Link Failure (RLF) and connect to a different cell, or directly reconnect to the new gNB, depending on the duration of the eviction timer. In the specific case of a 7.2 gNB, the re-deployment of a DU triggers an RU reset to accommodate the new DU MAC address (alternatively, the DU MAC can be spoofed, although this approach would not be scalable without

resorting to additional middleware components, as discussed in [37]).

VII. CONCLUSIONS AND FUTURE WORK

Starting from the Open RAN principles of disaggregation and standardization, we proposed AutoRAN, an open automation framework, which leverages cloud computing and virtualization techniques to seamlessly deploy, reconfigure, and test heterogeneous private 5G RANs and related components. We showcased the building blocks of AutoRAN, highlighting its advantages with respect to traditional deployment techniques, which are often monolithic and designed for highly experienced users. We experimentally evaluated the capabilities of AutoRAN, showing how the virtualization and automation functionalities that it offers introduce enhanced flexibility and seamless deployment and testing capabilities that take in input simple high-level intents expressed in natural language, instead of complex and detailed configurations. In future works, we will extend the same approach to manage additional NICs and hardware combinations (including RU configuration through M-Plane), as well as the automatic deployment of auxiliary components to the RAN.

ACKNOWLEDGMENTS

The authors would like to express their gratitude to Jing Xu, Anupa Kelkar, and Chris Dick from NVIDIA Corporation for their feedback on NVIDIA ARC. The authors disclose that AI tools (ChatGPT, Claude) have been used to perform minor edits and reformulations of the text.

REFERENCES

- [1] A. Narayanan, M. I. Rochman, A. Hassan, B. S. Firmansyah, V. Sathya, M. Ghosh, F. Qian, and Z.-L. Zhang, "A Comparative Measurement Study of Commercial 5G mmWave Deployments," in *IEEE Conference on Computer Communications*, 2022, pp. 800–809.
- [2] E. Dahlman, S. Parkvall, and J. Skold, *5G NR: The Next Generation Wireless Access Technology*. Academic Press, 2020.
- [3] Uptime Intelligence, "Annual outage analysis 2024," <https://datacenter.uptimeinstitute.com/rs/711-RIA-145/images/2024.Resiliency.Survey.ExecSum.pdf>, Uptime Intelligence, Tech. Rep., 2024, online; accessed 14 April 2025.
- [4] 3GPP, "5G for Industry 4.0," <https://www.3gpp.org/technologies/tsn-v-lan>, 2024, online; accessed 14 April 2025.
- [5] NEC Corporation, "Annual outage analysis 2024," https://www.nec.com/en/global/solutions/5g/download/pdf/Moving_to_Open_RAN.pdf, NEC Corporation, Tech. Rep., 2021, online; accessed 14 April 2025.
- [6] Red Hat, "OpenShift," <https://www.redhat.com/en/technologies/cloud-computing/openshift>, online; accessed 24 August 2025.
- [7] F. Kaltenberger, T. Melodia, I. Ghauri, M. Polese, R. Knopp, T. T. Nguyen, S. Velumani, D. Villa, L. Bonati, R. Schmidt, S. Arora, M. Irazabal, and N. Nikaiein, "Driving innovation in 6G wireless technologies: The OpenAirInterface approach," *Computer Networks*, vol. 269, p. 111410, 2025. [Online]. Available: <https://www.sciencedirect.com/science/article/pii/S1389128625003779>
- [8] N. Nikaiein, M. K. Marina, S. Manickam, A. Dawson, R. Knopp, and C. Bonnet, "OpenAirInterface: A flexible platform for 5G research," *ACM SIGCOMM Computer Communication Review*, vol. 44, no. 5, pp. 33–38, 2014.
- [9] D. Villa, I. Khan, F. Kaltenberger, N. Hedberg, R. S. da Silva, S. Maxenti, L. Bonati, A. Kelkar, C. Dick, E. Baena, J. M. Jornet, T. Melodia, M. Polese, and D. Koutsonikolas, "X5G: an Open, Programmable, Multi-vendor, End-to-end, Private 5G O-RAN Testbed with NVIDIA ARC and OpenAirInterface," *IEEE Transactions on Mobile Computing*, pp. 1–18, 2025.
- [10] A. Kelkar and C. Dick, "NVIDIA Aerial GPU Hosted AI-on-5G," in *2021 IEEE 4th 5G World Forum (5GWF)*, 2021, pp. 64–69.
- [11] SRS, "srsRAN," <https://www.srsran.com/5g>, 2024, online; accessed 11 April 2025.
- [12] P. Bahl, M. Balkwill, X. Foukas, A. Kalia, D. Kim, M. Kotaru, Z. Lai, S. Mehrotra, B. Radunovic, S. Saroiu, C. Settle, A. Verma, A. Wolman, F. Y. Yan, and Y. Zhang, "Accelerating Open RAN Research Through an Enterprise-scale 5G Testbed," in *Proceedings of the 29th Annual International Conference on Mobile Computing and Networking*, ser. ACM MobiCom '23. Madrid, Spain: Association for Computing Machinery, 2023.
- [13] L. Bonati, M. Polese, S. D'Oro, S. Basagni, and T. Melodia, "NeutRAN: An Open RAN Neutral Host Architecture for Zero-Touch RAN and Spectrum Sharing," *IEEE Transactions on Mobile Computing*, pp. 1–13, August 2023.
- [14] L. Bonati, M. Polese, S. D'Oro, P. B. del Prever, and T. Melodia, "5G-CT: Automated Deployment and Over-the-Air Testing of End-to-End Open Radio Access Networks," *IEEE Communications Magazine*, vol. 63, no. 1, pp. 155–160, 2025.
- [15] F. Mancini, L. Tamiano, and G. Bianchi, "5GShell: a plug-and-play framework for automating the deployment of 5G cellular networks," in *2023 26th Conference on Innovation in Clouds, Internet and Networks and Workshops (ICIN)*, 2023, pp. 39–41.
- [16] O. Arouk and N. Nikaiein, "5G Cloud-Native: Network Management & Automation," in *NOMS 2020 - 2020 IEEE/IFIP Network Operations and Management Symposium*, 2020, pp. 1–2.
- [17] L. L. Schiavo, G. Garcia-Aviles, A. Garcia-Saavedra, M. Gramaglia, M. Fiore, A. Banchs, and X. Costa-Perez, "CloudRIC: Open Radio Access Network (O-RAN) Virtualization with Shared Heterogeneous Computing," in *Proceedings of the 30th Annual International Conference on Mobile Computing and Networking*, ser. ACM MobiCom '24. Washington D.C., DC, USA: Association for Computing Machinery, 2024, p. 558–572.
- [18] A. Gudipati, D. Perry, L. E. Li, and S. Katti, "SoftRAN: software defined radio access network," in *Proceedings of the Second ACM SIGCOMM Workshop on Hot Topics in Software Defined Networking*, ser. HotSDN '13. Hong Kong, China: Association for Computing Machinery, 2013, p. 25–30.
- [19] S. D'Oro, L. Bonati, M. Polese, and T. Melodia, "OrchestRAN: Network Automation through Orchestrated Intelligence in the Open RAN," in *IEEE Conference on Computer Communications (INFOCOM)*. IEEE Press, 2022, p. 270–279.
- [20] A. Mohammadi and N. Nikaiein, "Athena: An Intelligent Multi-x Cloud Native Network Operator," *IEEE Journal on Selected Areas in Communications*, vol. 42, no. 2, pp. 460–472, 2024.
- [21] M. McManus, T. Rinchen, A. Dey, S. Thota, Z. Zhang, J. Hu, X. Wang, M. Ji, N. Mastronarde, E. S. Bentley, M. Medley, and Z. Guan, "Cloud-Based Federation Framework and Prototype for Open, Scalable, and Shared Access to NextG and IoT Testbeds," 2024. [Online]. Available: <https://arxiv.org/abs/2408.14460>
- [22] Y. Wei, X. Xie, Y. Zuo, T. Hu, X. Chen, K. Chi, and Y. Cui, "Leveraging LLM Agents for Translating Network Configurations," 2025. [Online]. Available: <https://arxiv.org/abs/2501.08760>
- [23] H. Zhou, C. Hu, Y. Yuan, Y. Cui, Y. Jin, C. Chen, H. Wu, D. Yuan, L. Jiang, D. Wu, X. Liu, C. Zhang, X. Wang, and J. Liu, "Large Language Model (LLM) for Telecommunications: A Comprehensive Survey on Principles, Key Techniques, and Opportunities," *IEEE Communications Surveys & Tutorials*, pp. 1–1, 2024.
- [24] O-RAN Alliance, "O-RAN Control, User and Synchronization Plane Specification," <https://www.o-ran.org/specifications>, O-RAN Alliance, Tech. Rep. O-RAN.WG4.CUS.0-R004-v16.01, March 2024, online; accessed 14 April 2025.
- [25] S. D'Oro, M. Polese, L. Bonati, H. Cheng, and T. Melodia, "dApps: Distributed Applications for Real-Time Inference and Control in O-RAN," *IEEE Communications Magazine*, vol. 60, no. 11, pp. 52–58, 2022.
- [26] O-RAN next Generation Research Group (nGRG), "dApps for Real-Time RAN Control: Use Cases and Requirements (Report ID: RR-2024-10)," <https://tinyurl.com/5n82pwpX>, October 2024.
- [27] A. Lacava, L. Bonati, N. Mohammadi, R. Gangula, F. Kaltenberger, P. Johari, S. D'Oro, F. Cuomo, M. Polese, and T. Melodia, "dApps: Enabling real-time AI-based Open RAN control," *Computer Networks*, vol. 269, p. 111342, 2025. [Online]. Available: <https://www.sciencedirect.com/science/article/pii/S1389128625003093>
- [28] "Prometheus," accessed 24 August 2025. [Online]. Available: <https://prometheus.io/>
- [29] "Observium," accessed 14 April 2025. [Online]. Available: <https://observium.org>
- [30] "OpenAirInterface for 7.2 split," online; accessed 7 October 2025. [Online]. Available: https://gitlab.eurecom.fr/oai/openairinterface5g/-/blob/develop/doc/ORAN_FH17.2_Tutorial.md#configure-your-server

- [31] “TrueNAS,” <https://www.truenas.com/>, 2024, online; accessed 12 September 2024.
- [32] NVIDIA, “GDRCopy,” <https://github.com/NVIDIA/gdrcopy>, 2024, online; accessed 12 September 2024.
- [33] M. Polese, L. Bonati, S. D’Oro, S. Basagni, and T. Melodia, “Understanding O-RAN: Architecture, Interfaces, Algorithms, Security, and Research Challenges,” *IEEE Communications Surveys & Tutorials*, vol. 25, no. 2, pp. 1376–1411, 2023.
- [34] E. Moro, M. Polese, A. Capone, and T. Melodia, “An Open RAN Framework for the Dynamic Control of 5G Service Level Agreements,” in *IEEE Conference on Network Function Virtualization and Software Defined Networks (NFV-SDN)*, Dresden, Germany, November 2023.
- [35] L. Bonati, M. Polese, S. D’Oro, S. Basagni, and T. Melodia, “OpenRAN Gym: AI/ML Development, Data Collection, and Testing for O-RAN on PAWR Platforms,” *Computer Networks*, vol. 220, pp. 1–11, January 2023.
- [36] G. Gemmi, M. Polese, P. Johari, S. Maxenti, M. Seltser, and T. Melodia, “Open6G OTIC: A Blueprint for Programmable O-RAN and 3GPP Testing Infrastructure,” in *IEEE 100th Vehicular Technology Conference*, 2024, pp. 1–5.
- [37] X. Foukas, T. S. Ukyab, B. Radunovic, S. Ratnasamy, and S. Shenker, “RANBooster: Democratizing advanced cellular connectivity through fronthaul middleboxes,” in *Proceedings of the ACM SIGCOMM 2025 Conference*, ser. SIGCOMM ’25. New York, NY, USA: Association for Computing Machinery, 2025, p. 742–757. [Online]. Available: <https://doi.org/10.1145/3718958.3754349>



Stefano Maxenti is a Ph.D. Candidate in Computer Engineering at the Institute for the Wireless Internet of Things (WIoT) at Northeastern University, under Prof. Tommaso Melodia. He received a B.Sc. in Engineering of Computing Systems in 2020 and a M.Sc. in Telecommunication Engineering in 2023 from Politecnico di Milano, Italy. His research is linked with AI applications for wireless communications and orchestration, integration, and automation of O-RAN networks.



Ravis Shirkhani is a Ph.D. Candidate in Computer Engineering at the Institute for the Wireless Internet of Things (WIoT) at Northeastern University, under Prof. Tommaso Melodia. She received a B.Sc. in Electrical Engineering (Communication Systems and Networks) in 2023 from Sharif University of Technology, Iran. Her research focuses on automation of O-RAN networks, power consumption across O-RAN components, and exploring optimization approaches for network energy efficiency.



Maxime Elkael is a Research Scientist at the Institute for the Wireless Internet of Things at Northeastern University. He received his Ph.D in Computer Science from Institut Polytechnique De Paris/Telecom SudParis in 2023. His research interest lies at the intersection of optimization theory, artificial intelligence and graph theory applied to next generation wireless networks, especially Open RAN networks.



Leonardo Bonati is an Associate Research Scientist at the Institute for the Wireless Internet of Things, Northeastern University, Boston, MA. He received a Ph.D. degree in Computer Engineering from Northeastern University in 2022. His main research focuses on softwareized approaches for the Open Radio Access Network (RAN) of the next generation of cellular networks, on O-RAN-managed networks, and on network automation, orchestration, and virtualization. He was awarded the 2024 Mario Gerla Award for Research in Computer Science. Leonardo

served as TPC co-chair for the IEEE DTwin 2025 workshop, as co-chair for the track on Testbeds, Experimentation and Datasets for Communications and Networking of IEEE CCNC 2025, and as guest editor of the special issue of Elsevier Computer Networks on Advances in Experimental Wireless Platforms and Systems.



Salvatore D’Oro is the CTO and co-founder of zTouch Networks, a company focused on the development of zero-touch automation solutions for O-RAN systems. He is also a Research Associate Professor at Northeastern University. He received his Ph.D. degree from the University of Catania and is an area editor of Elsevier Computer Communications journal. He serves on the TPC of IEEE INFOCOM, IEEE CCNC & ICC and IFIP Networking. He is one of the contributors to OpenRAN Gym, the first open-source research platform for AI/ML applications in

the Open RAN. His research interests include optimization, AI & network slicing for NextG Open RANs.



Tommaso Melodia is the William Lincoln Smith Chair Professor with the Department of Electrical and Computer Engineering at Northeastern University in Boston. He is also the Founding Director of the Institute for the Wireless Internet of Things and the Director of Research for the PAWR Project Office. He received his Ph.D. in Electrical and Computer Engineering from the Georgia Institute of Technology in 2007. He is a recipient of the National Science Foundation CAREER award. Prof. Melodia has served as Associate Editor of IEEE Transactions on

Wireless Communications, IEEE Transactions on Mobile Computing, Elsevier Computer Networks, among others. He has served as Technical Program Committee Chair for IEEE INFOCOM 2018, General Chair for IEEE SECON 2019, ACM Nanocom 2019, and ACM WUWnet 2014. Prof. Melodia is the Director of Research for the Platforms for Advanced Wireless Research (PAWR) Project Office, a \$100M public-private partnership to establish four city-scale platforms for wireless research to advance the US wireless ecosystem in years to come. Prof. Melodia’s research on modeling, optimization, and experimental evaluation of Internet-of-Things and wireless networked systems has been funded by the National Science Foundation, the Air Force Research Laboratory the Office of Naval Research, DARPA, and the Army Research Laboratory. Prof. Melodia is a Fellow of the IEEE and a Distinguished Member of the ACM.



Michele Polese is a Research Assistant Professor at the Institute for the Wireless Internet of Things, Northeastern University, Boston, since October 2023. He received his Ph.D. at the Department of Information Engineering of the University of Padova in 2020. He then joined Northeastern University as a research scientist and part-time lecturer in 2020. During his Ph.D., he visited New York University (NYU), AT&T Labs in Bedminster, NJ, and Northeastern University. His research interests are in the analysis and development of protocols and architectures for

future generations of cellular networks (5G and beyond), in particular for millimeter-wave and terahertz networks, spectrum sharing and passive/active user coexistence, open RAN development, and the performance evaluation of end-to-end, complex networks. He has contributed to O-RAN technical specifications and submitted responses to multiple FCC and NTIA notice of inquiry and requests for comments, and is a member of the Committee on Radio Frequency Allocations of the American Meteorological Society (2022–2024). He is PI and co-PI in research projects on 6G funded by the NTIA, the O-RAN ALLIANCE, U.S. NSF, OUSD, and MassTech Collaborative, and was awarded with several best paper awards and the 2022 Mario Gerla Award for Research in Computer Science. Michele is serving as TPC co-chair for WNS3 2021–2022, as an Associate Technical Editor for the IEEE Communications Magazine, as a Guest Editor in an IEEE JSAC Special Issue on Open RAN, and has organized the Open 5G Forum in Fall 2021 and the NextGenRAN workshop at Globecom 2022.